Department of Chemical Engineering
University of California, Santa Barbara

CH E 180A. Chemical Engineering Laboratory

Compressibility Factor and Second Virial Coefficient of Nonideal Carbon Dioxide and Helium Between 15-35°C Determined by the Burnett Method

Sean Shen, Melody Spann, Yulun Wu
Group 8T

Experiment Conducted between April 23 and April 30, 2024
Report Submitted on May 7, 2024

1 Abstract

The Ideal Gas Law is widely recognized for describing the physical properties of gases, such as density and volume, under conditions of high temperature and low pressure. However, it falls short in accurately depicting the behavior of real gases under low temperature and high pressure conditions. To address this discrepancy, scientists employ compressibility factors (Z) and second virial coefficients (B), which provide a more precise characterization of real gases. These measurements are critical in industrial applications, enhancing the safety and optimizing the conditions for reactor design. This report investigates the compressibility factors and second virial coefficients of gases at low temperatures (15-35°C) using the Burnett method. We conducted experiments to record gas expansion at three distinct temperatures for both carbon dioxide and helium. Each gas underwent two trials. For helium, temperatures were recorded at $21.3 \pm 0.05°C$, $27.0 \pm 0.05°C$, and $34.0 \pm 0.05°C$. For carbon dioxide, the temperatures were $15.3 \pm 0.05°C$, $21.1 \pm 0.05°C$, and $27.0 \pm 0.05°C$. The compressibility factors for helium were consistently above 1 and increased with rising pressure, whereas those for carbon dioxide were generally below 1 and decreased as pressure increase. The second virial coefficients for helium were $17.38 \pm 7.10 \frac{\text{cm}^3}{\text{mol}}$, $25.34 \pm 7.24 \frac{\text{cm}^3}{\text{mol}}$, and $15.56 \pm 7.41 \frac{\text{cm}^3}{\text{mol}}$ at 21.3, 27.0, and $34.0°C$, respectively. For carbon dioxide, the coefficients were $-168.31 \pm 6.96 \frac{\text{cm}^3}{\text{mol}}$, $-175.62 \pm 7.10 \frac{\text{cm}^3}{\text{mol}}$, and $-172.64 \pm 7.24 \frac{\text{cm}^3}{\text{mol}}$ at 15.3, 21.1, and $27.0°C$, respectively. This report also discusses the trends between molecular properties and the observed values of compressibility factors and second virial coefficients, highlighting how factors like intermolecular forces and molecular size influence these properties. Understanding these relationships is crucial for predicting molecular characteristics of gases based on changes in volume and pressure, thus providing deeper insight into the behavior of real gases.

2 Introduction

The ideal gas equation applies to gases at high temperatures and low pressures, where it is assumed volume, intermolecular forces, and collisions of the atoms are negligible. Equation 1 shows the ideal gas law where p is absolute pressure in Psia, V is the volume occupied by the gas in L, n is the total moles, R is the gas constant $1.206 \frac{\text{L Psia}}{\text{mol K}}$, and T is the absolute temperature in K:

$$pV = nRT \tag{1}$$

The volume and interactions of real gases significantly affect its properties, and thus Equation 1 is modified by the Z-factor, a dimensionless value that accounts for the compressibility of nonideal gases to generate Equation 2:

$$pV = ZnRT \tag{2}$$

The Burnett method determines Z by measuring the pressure change of a gas as it expands from one vessel into a second vessel isothermally to reach mechanical equilibrium [**1**]. The vessels are hereon referred to as cell "A," the initial vessel containing the gas, and cell "B," the vessel into which the gas expands. The volume of the cells are unknown and thus a dimensionless constant N is defined as the apparatus constant in Equation 3, where V_A

and V_B are the volumes of cells "A" and "B" respectively [**2**]:

$$N = \frac{V_A + V_B}{V_A} \tag{3}$$

After the r-th expansion of the gas from cell "A" to "B," the moles and volume can be simplified to represent the change in pressure as seen in Equation 4:

$$\frac{p_{r-1}}{p_r} = \frac{NZ_{r-1}}{Z_r} \tag{4}$$

where the subscripts note the number of expansions the system has undergone, $r = 0$ denotes the initial conditions of the system [**2**]. For ideal gases Z is 1, thus the limit of Equation 4 should approach N, as pressure approaches zero. Equation 4 can be rearranged to relate the initial conditions of cell "A" to the conditions of the system after the r-th expansion through Equation 5 where Z_0 and p_0 are the compressibility and pressure within cell "A" before the first expansion [**3**]:

$$(\frac{Z_0}{p_0})p_r N^r = Z_r \tag{5}$$

Similar to the apparatus constant, the Z-factor of the gas at any pressure is determined by taking the limit of Equation 5 as pressure approaches zero and the number of expansions, r, increases [**3**]. The Z-factor of ideal gases is 1, so the initial Z factor to initial pressure can be determined graphically [**4**]. The Virial expansion equation uses temperature-dependent coefficients to correct for the nonideality of gases [**5**]. The second virial coefficient, B, is a temperature-dependent value with units of mL mol^{-1} that is calculated from the Z-factor using Equation 6 [**5**]:

$$Z = 1 + \frac{Bp}{RT} \tag{6}$$

The Boyle temperature is where the second virial coefficient becomes zero and thus reaches ideality, over a given pressure range [**6**]. For gases near critical temperature, the compressibility factor becomes significantly large, and thus small changes result in large changes in overall volume [**7**].

3 Method

The Burnett method is one of the simplest ways to measure the nonideality of gases and the apparatus is displayed in Figure 1. While carbon dioxide and helium were both measured using the Burnett apparatus, the instruments differed, thus the apparatus constant, and error associated with absolute temperature and absolute pressure differed. The method varies the volume and the moles of the gas of interest, while measuring the absolute temperature and the absolute pressure [**1**]. For simplicity, temperature control was used to heat up the water bath and the cells to ensure that the expansion of the gas occurred under isothermal conditions. The gauge pressure of carbon dioxide was measured at $15.25 \pm 0.01°C$, $21.07 \pm 0.01°C$, and $27.00 \pm 0.01°C$. The gauge pressure of helium was measured at $21.3 \pm 0.1°C$, $27.0 \pm 0.1°C$, and $34.0 \pm 0.1°C$. At each temperature, two trials were conducted to ensure the consistency of the results. The system was purged

twice prior to each measurement to ensure proper replicates. Purging involved filling cells "A" and "B" with gas using valve one (V-1) and opening valve five (V-5) to release the pressure in the system and closing once all the gas had been released. Valve three (V-3) was then opened to evacuate the system and achieve as close to a vacuum as possible. It is vital to ensure that valve four (V-4) was closed after the gas was released by V-5, as subjecting the pressure gauge to a vacuum would lead to negative readings, ultimately distorting the readings and damaging the instrument. Since the two gases used different Burnett setups, the apparatus constant was determined for each. First, cell "A" was filled with gas, ensuring that only valve four (V-4) was open. This allowed us to measure the exact pressure of the gas within cell "A." Cell "B" was evacuated to ensure a proper vacuum. Then valve two (V-2) was opened to isothermally expand the gas into cell "B," until equilibrium was reached. The pressure in cell "A" was recorded and V-2 was closed and the experiment was repeated until the pressure in cell "A" remained between 10-20 PSIG. Several assumptions were made to ensure efficient measurements. It was assumed that the inside of the metal cells and the gas had the same temperature as the water bath. The pressure gauge only measures the pressure within cell "A," and thus when the pressure remained constant, it was assumed that equilibrium was reached. Mathematically, equilibrium can only be achieved after an infinite amount of time, but this is not feasible in the lab.

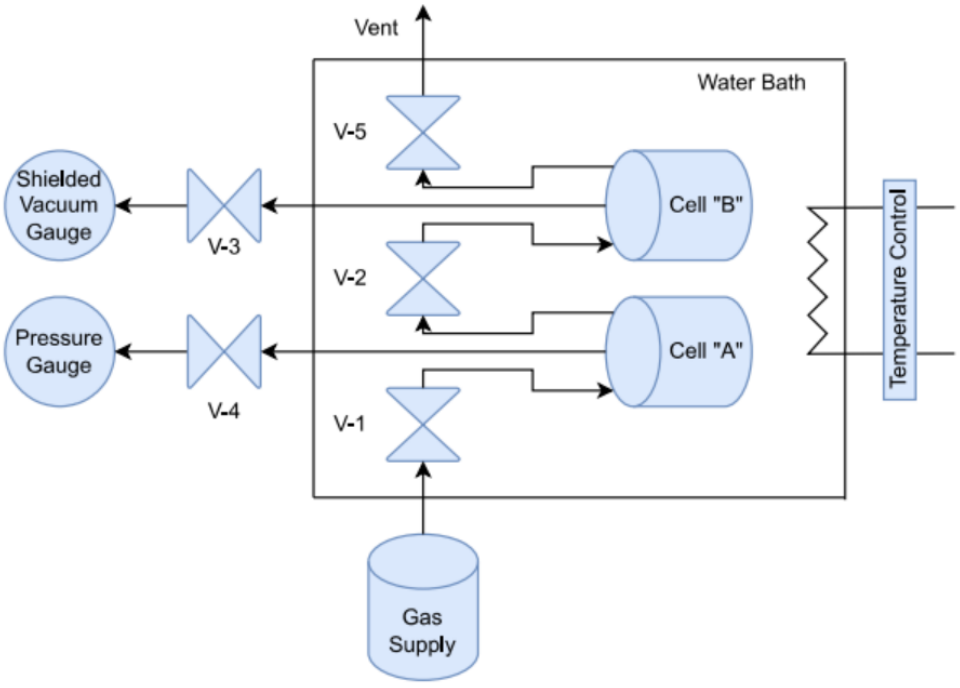

Figure 1: The general Burnett apparatus setup used to determine the equilibrium pressure in cell "A" at various temperatures for carbon dioxide and helium. The gasses were tested using different instruments to ensure no cross contamination.

4 Results and Discussion

4.1 Determination of apparatus Constant

The apparatus constant N, representing the ratio of volumes, should ideally remain consistent throughout the experiment. A $\frac{P_{r-1}}{P_r}$ vs. P_r graph was plotted, and linear extrapolation was performed on the models to determine N for each trial and temperature (see Appendix C.1–C.6). By calculating the averaged N for each apparatus, N for the He-measuring device, 1.98 ± 0.01, aligns well with the expected value of 2, which is derived from Equation 3; however, N for the CO_2-measuring device, 1.45 ± 0.01, is significantly lower than the expected value. This might be caused by the tubes and fittings connected to the cells, which could affect V_A to be larger than the imagined volume.

4.2 Determination of Compressibility factors

Compressibility factors (Z_r) at all pressures, P_r, were calculated using Equation 5. Figure 2 illustrates the relationship between the compressibility factors and pressure for each expansion number for both carbon dioxide and helium.

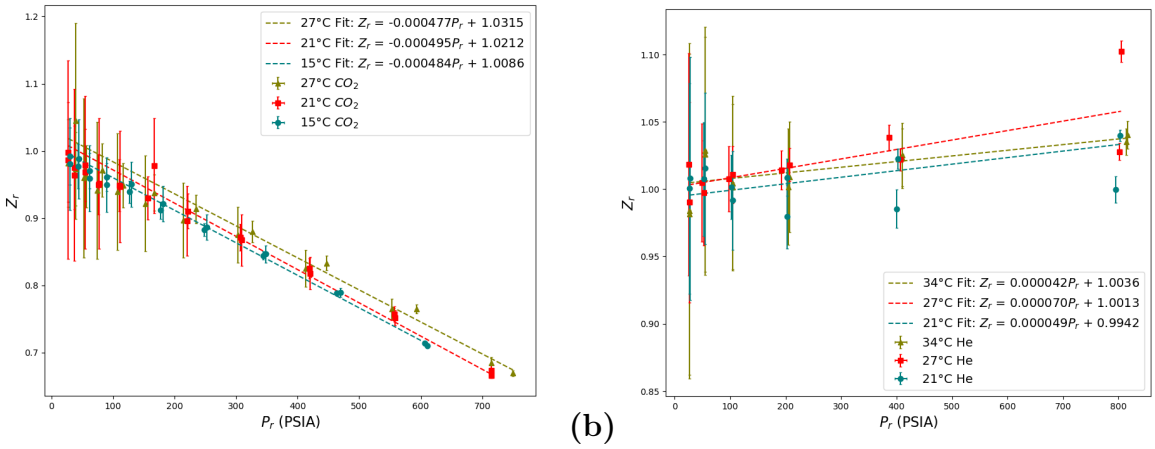

Figure 2: The compressibility factor Z_r, as a function of the pressure of (a) carbon dioxide and (b) helium at the tested temperatures. The vertical error bars represent the propagated error of Z_r calculated in Appendix B, and the horizontal error bar represents the measurement uncertainties of pressure (1 psi for carbon dioxide and 2 psi for helium due to different apparatus). The trendline for each temperature is indicated in the legend.

According to Figure 2, Z_r for both gasses approaches 1 as pressure decreases, supporting the ideal gas law that real gasses behave like ideal gasses at low pressures. At low pressures, larger volume occupied by the gas molecules allows them to remain further apart, causing weaker intermolecular forces [10]. Linear regression analysis reveals that Z_r of carbon dioxide decreases markedly with increasing pressure, whereas Z_r of helium increases only slightly. According to equation 2, if Z_r is smaller than 1 which means that the gasses decrease more volume than ideal gas when pressure increases and vice versa

These differences can be attributed to the unique molecular properties of the gases. Carbon dioxide, a binary compound consisting of one carbon atom and two oxygen atoms, exhibits relatively strong intermolecular forces due to its molecular size and atomic composition. As pressure increases, the reduction in volume occupied by carbon dioxide

molecules enhances these intermolecular forces, causing a greater deviation from ideal gas behavior and a decrease in Z_r. A reasonable assumption arises that when the pressure increases to a certain level, the distance between the carbon dioxide molecules becomes really small, and the attractive forces would become repulsive and cause Z_r to increase. However, it should be noted that testing the pressure level for carbon dioxide is not feasible under the testing range of temperature (15–35$°C$) due to safety concerns, as carbon dioxide would transition to a liquid state.

Conversely, helium, with small molecular size and a dominance of repulsive forces [**8**], displays a Z_r greater than 1, as these forces prevent volume reduction relative to ideal gases. As a noble gas, helium possesses weak London dispersion forces, making helium gas less susceptible to changes in compressibility factor compared to carbon dioxide.

Ultimately, the sign of the linear regression between Z_r and P_r indicates whether repulsive or attractive forces are predominant under specific temperature and pressure conditions. The magnitude of this slope further suggests the strength of the intermolecular forces involved.

4.3 Determination of The Second Virial Coefficient, B

The second virial coefficients of carbon dioxide and helium were calculated using Equation 6. Figure 3 presents the second virial coefficients for both gases at the tested temperatures.

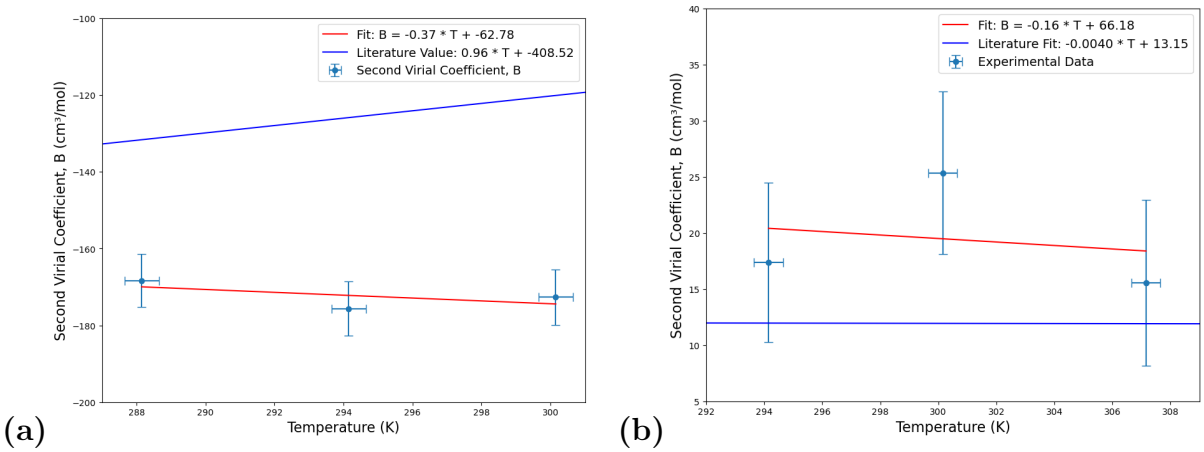

Figure 3: The second virial coefficient B, as a function of the pressure of (a) carbon dioxide and (b) helium at the tested temperatures. The horizontal error bar represents the measurement uncertainty of the temperature, and the vertical error bar represents the propagated error for B as calculated in appendix B. The Chi-squared regression line is plotted, and the formulas for both gasses are shown in the legend. The literal value of second virial coefficients is also plotted.

As suggested by Figure 3, the second virial coefficients of helium are closer to zero compared to those of carbon dioxide. According to Equation 6, a second virial coefficient closer to 0 indicates that the actual compressibility factor Z is closer to 1, supporting the idea that helium behaves more ideally than carbon dioxide due to weak intermolecular forces. Additionally, the signs of the second virial coefficients for both gases are consistent with their molecular interactions. At lower temperatures, carbon dioxide exhibits

attractive forces leading to negative second virial coefficients, which reduce Z below 1. In contrast, helium predominantly exhibits repulsive forces, resulting in positive second virial coefficients, thus increasing Z above 1. This trend of second virial coefficients decreasing with temperature supports the theory that gases behave more ideally at higher temperatures.

The second virial coefficients for helium are presented in Table C.1 A t-test comparing these values to those in the literature yielded a p-value of 0.067, indicating no statistically significant difference from the literature values. The discrepancy might be attributed to calculation errors in Equation 6, because it is a truncated version of the virial equation of state. In contrast, the second virial coefficients for carbon dioxide, listed in Table C.2, show a negative correlation with temperature—a result that contradicts expectations. The corresponding p-value of 0.73 suggests that the experimental data significantly deviates from the literature values. One potential source of error could be inconsistent temperatures of the water bath. In addition, the thermocontroller has inadequate stirring, and the thermometer only measures from a specific region of water, potentially misrepresenting the actual temperature of the cells and leading to inaccurate calculations of the second virial coefficient. This error could be minimized by more thoroughly stirring the water tank and ensuring that experimental temperatures are set above room temperature. One other potential source of error is the failure to completely evacuate cell B before performing another expansion which might lead to higher pressure readings from cell A, thereby the second virial coefficient could be underestimated.

5 Conclusions

In our study, we determined the compressibility factors and the second virial coefficients of carbon dioxide and helium gases between 15–35°C using the Burnett method. The experimental results corroborate established theories suggesting that helium behaves more ideally than carbon dioxide, due to its smaller molecular size and weaker intermolecular forces. We confirmed that the compressibility factors for helium increase with pressure and consistently exceed 1, whereas those for carbon dioxide are predominantly below 1 and decrease with increasing pressure. Additionally, the calculated second virial coefficients for helium closely align with literature values. In contrast, those for carbon dioxide are significantly lower, likely due to inaccuracies in the recorded temperature and pressure. We recommend allowing cell B ample time to fully evacuate and for the vacuum gauge to reach the lowest residual pressure before taking measurements. Furthermore, waiting for the expanded gas to fully equilibrate before recording pressure readings may improve accuracy. Determining higher-order virial coefficients could also significantly reduce errors associated with truncating the equation. To enhance data accuracy, using a more effective thermocontroller to maintain a consistent temperature in the water bath is advisable. Increasing the robustness of our conclusions may be achieved by conducting additional trials at various temperatures and with different gases.

References

[1] Burnett, E. S., J. App. Mech. 1936, 3(4), A136-A140.

[2] Silberberg, I. H., et al., J. Chem. Eng. Data 1959, 4, 314-323.

[3] Silberberg, I. H., et al., J. Chem. Eng. Data 1959, 4, 323-329.

[4] UC Santa Barbara, Department of Chemical Engineering; ChE 180A: Chemical Engineering Laboratory Manual: Compressibility Factor and Second Virial Coefficients; UC Santa Barbara: Santa Barbara, Updated April 2018.

[5] Demirel, Y.; Gerbaud, V. Nonequilibrium Thermodynamics: Transport and Rate Processes in Physical, Chemical and Biological Systems, 4th ed.; Elsevier Science LTD, 2019, 62-65.

[6] Wisniak, J. Interpretation of the Second Virial Coefficient, J. Chem. Educ. 1999, 76 (5), 671. DOI: 10.1021/ed076p671.

[7] LaNasa, P. J.; Upp, E. L. Fluid Flow Measurement, 3rd ed.; Elsevier Science LTD, 2014, 83-87.

[8] Rackers, J. A.; Ponder, J. W. Classical Pauli repulsion: An anisotropic, atomic multipole model, J. Chem. Phys. 2019, 150(8), 084104. DOI: 10.1063/1.5081060.

[9] McCarthy, R. D. Thermodynamic Properties of Helium 4 from 2 to 1500 K at Pressures to 108 Pa, J. Phys. Chem. Ref. Data 1973, 2, 923–1042. DOI: 10.1063/1.3253133.

[10] Tenny, K. M.; Cooper, J. S. Ideal Gas Behavior. StatPearls, StatPearls Publishing, November 28, 2022.

[11] Dadson, R. S.; Evans, E. J.; King, J. H. The second virial coefficient of carbon dioxide. Proc. Phys. Soc. 1967, 92 (4), 1115. DOI: 10.1088/0370-1328/92/4/337.

A Raw Data

Table A.1: Raw Data of Pressures in Each Expansion of Helium

Pressure (psig) ± 2						
Temperature (°C) ± 0.5	34.0 °C		27.0 °C		21.3 °C	
Expansion #	Trial 1	Trial 2	Trial 1	Trial 2	Trial 1	Trial 2
0	802	800	790	787	788	780
1	396	396	372	392	388	385
2	190	192	178	192	188	188
3	90	90	83	90	88	90
4	40	40	35	38	38	40
5	12	12	11	12	12	13

Table A.2:Raw Data of Pressures in Each Expansion of Carbon Dioxide

Presure (psig) ± 1						
Temperature (°C) ± 0.5	27.00 °C		21.07 °C		15.25°C	
# Expansion	1st trial	2nd trial	1st trial	2nd trial	1st trial	2nd trial
0	735	700	700	700	596	592
1	578	538	542	544	455	449
2	432	398	405	406	334	329
3	312	288	292	294	238	234
4	220	200	207	206	167	163
5	152	138	142	152	115	112
6	102	93	96	97	75	75
7	68	60	62	63	48	48
8	42	38	40	40	30	29
9	25	25	23	23	16	16
10	13		12	12		

B Sample Calculations

B.1 Apparatus Constant

Apparatus Constant N Definition:

$$N = \lim_{p \to 0} \frac{P_{r-1}}{P_r}$$

Finding the Y-Intercept: N can be found by finding the y-intercept of the linear regression line for the plot of $\frac{P_{r-1}}{P_r}$ and P_{r-1}.

Sample Calculation for $\frac{P_{r-1}}{P_r}$:

$$\frac{P_0}{P_1} = \frac{735}{578} = 1.271$$

Sample Error Calculation $\frac{P_{r-1}}{P_r}$:

$$\delta = \sqrt{\left(\frac{1}{578}\right)^2 \times 2 + \left(\frac{-735}{578^2}\right)^2 \times 2} = 0.003$$

Line of Best Fit Calculation:

$$\text{Slope} = \frac{\sum_{i=1}^{n}(x_i - \bar{x})(y_i - \bar{y})}{\sum_{i=1}^{n}(x_i - \bar{x})^2} = -5.86 \times 10^{-6}$$

Y-Intercept Calculation:

$$\text{Y-intercept} = \bar{y} - \text{slope} \times \bar{x} = 1.52$$

Sample Calculation for N:

$$\sqrt{\frac{\sum \delta N_i}{n}} = 0.01$$

Table B.1: Apparatus Constant of Helium for each Trial and Temperature

	Trial 1			Trial 2			Average
Temperature (°C) ± 0.5	34.0	27.0	21.3	34.0	27.0	21.3	
Apparatus Constant, N	1.98 ± 0.04	1.94 ± 0.04	1.96 ± 0.01	1.98 ± 0.01	1.93 ± 0.01	1.94 ± 0.02	1.96 ± 0.01

Table B.2: Apparatus Constant of Carbon Dioxide for each Trial and Temperature

	Trial 1			Trial 2			Average
Temperature (°C) ± 0.5	27.0	21.1	15.3	27.0	21.1	15.3	
Apparatus Constant, N	1.460 ± 0.008	1.420 ± 0.022	1.450 ± 0.009	1.450 ± 0.021	1.450 ± 0.010	1.440 ± 0.004	1.445 ± 0.010

B.2 Compressibility Factor

Compressibility Factor Z_0 Definition:

$$Z_0 = \lim_{P \to 0} \frac{P_0}{Z_0}$$

Finding the Y-Intercept:

Z_0 can be found by finding the y-intercept of the linear regression for the plot of P_r and N^r.

Line of Best Fit Calculation:

$$\text{Slope} = \frac{\sum_{i=1}^{n}(x_i - \bar{x})(y_i - \bar{y})}{\sum_{i=1}^{n}(x_i - \bar{x})^2} = -0.839$$

Y-Intercept Calculation:

$$\text{Y-intercept} = \bar{y} - \text{slope} \times \bar{x} = 1174$$

Sample Error Calculation for $P_r N^r$:

$$\delta = \sqrt{(1.52)^2 \cdot 1 + (1.52 \cdot 1 \cdot 578)^2 \cdot 0.0028^2} = 2.22$$

Calculation of Z_0 Using Y-Intercept:

$$Z_0 = \frac{P_0}{y - \text{intercept}} = \frac{735}{1174} = 0.626$$

Sample Error Calculation for Z_0:

$$\delta = \sqrt{\left(\frac{1}{1174}\right)^2 + \left(\frac{-735}{1174^2}\right)^2 \cdot 2.22^2} = 0.001$$

Calculation of Z_r Using $P_r N^r$ and Z_0:

$$Z = P_r N^r \times \frac{Z_0}{P_0} = 878.56 \times \frac{0.626}{735} = 0.75$$

Sample Error Calculation for Z:

$$\delta = \sqrt{(1.54 \times 0.655)^2 + (578 \times 1.54 \times 0.655)^2 \times 0.002^2 + (1.54 \times 578 \times 1)^2 \times 0.002^2 + (1.54 \times 578 \times 0.655)^2 \times 0.002^2} = 0.03 \quad \textit{dotted}$$

B.3 Second Virial Coefficient

Second Virial Coefficient is found by plotting Z_r vs P_r:

Line of Best Fit Calculation:

$$\text{Slope} = \frac{\sum_{i=1}^{n}(x_i - \bar{x})(y_i - \bar{y})}{\sum_{i=1}^{n}(x_i - \bar{x})^2} = -0.00049379\,\text{psi}^{-1}$$

Y-intercept Calculation:

$$\text{Y-intercept} = \bar{y} - \text{slope} \times \bar{x} = 1.0000$$

Sample calculation for Second Virial Coefficient:

$$B = -0.00049379 \times 8.314 \times (273.15 + 27.00) \times \frac{14.696\,\text{psi}}{101325} \times 10^6\,\text{cm}^3/\text{m}^3 = -178.72\,\frac{\text{cm}^3}{\text{mol}}$$

Sample error calculated for B:

$$\delta B = \sqrt{(-0.00049379 \times 1205.85)^2 \times 0.5^2 + (1205.85 \times 300.15)^2 \times 0.005^2} = 7.2\,\frac{\text{cm}^3}{\text{mol}}$$

C Supplemental Graph

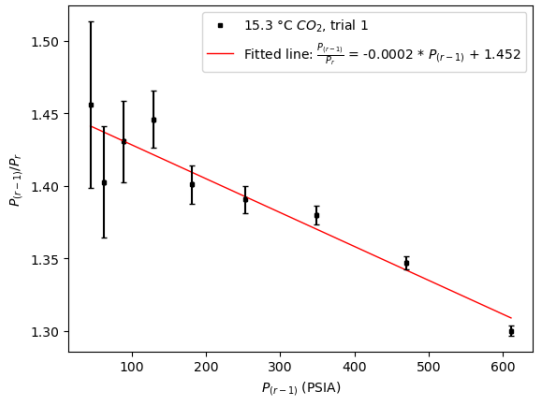

(a)

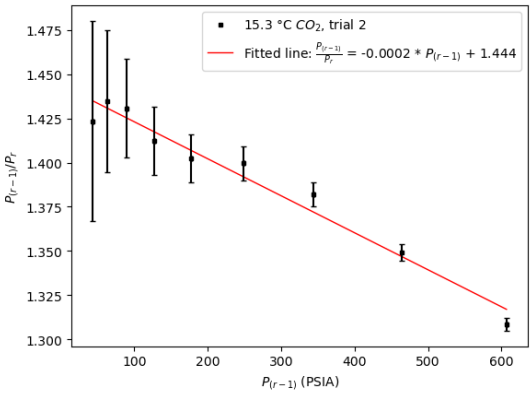

(b)

Figure C1: $\frac{P_{r-1}}{P_r}$ as a function of P_{r-1} of carbon dioxide at $15.3°C$. The linear model is fitted to the (a) first trial (b) second trial to determine the pressure decrease as pressure approaches zero. The vertical error bars represent the propagated error of $\frac{P_{r-1}}{P_r}$ and the horizontal error bar represents the measured uncertainty of the pressure

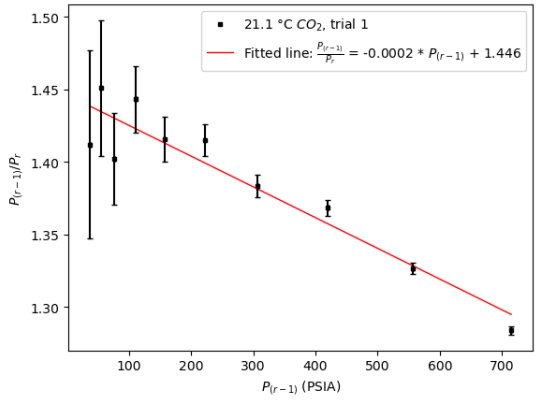

(a)

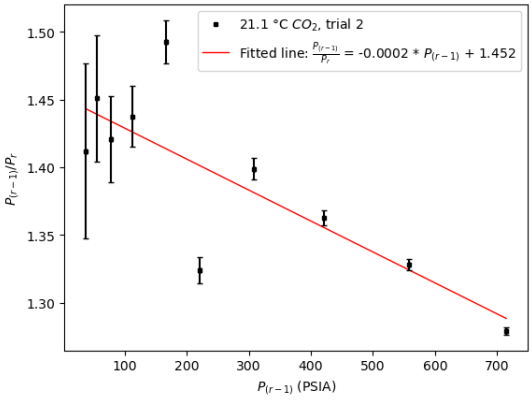

(b)

Figure C2: $\frac{P_{r-1}}{P_r}$ as a function of P_{r-1} of carbon dioxide at $21.1°C$. The linear model is fitted to the (a) first trial (b) second trial to determine the pressure decrease as pressure approaches zero. The vertical error bars represent the propagated error of $\frac{P_{r-1}}{P_r}$ and the horizontal error bar represents the measured uncertainty of the pressure

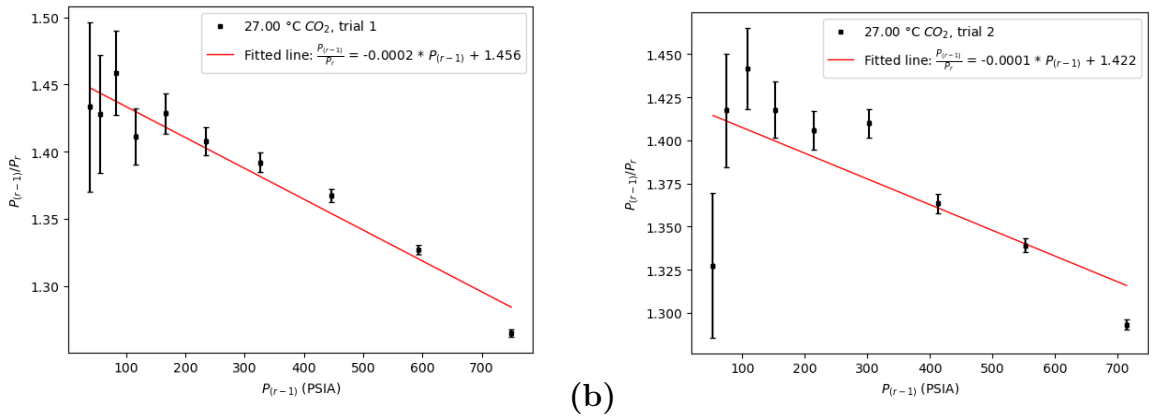

(a) (b)

Figure C3: $\frac{P_{r-1}}{P_r}$ as a function of P_{r-1} of carbon dioxide at 27.0°C. The linear model is fitted to the (a) first trial (b) second trial to determine the pressure decrease as pressure approaches zero. The vertical error bars represent the propagated error of $\frac{P_{r-1}}{P_r}$ and the horizontal error bar represents the measured uncertainty of the pressure

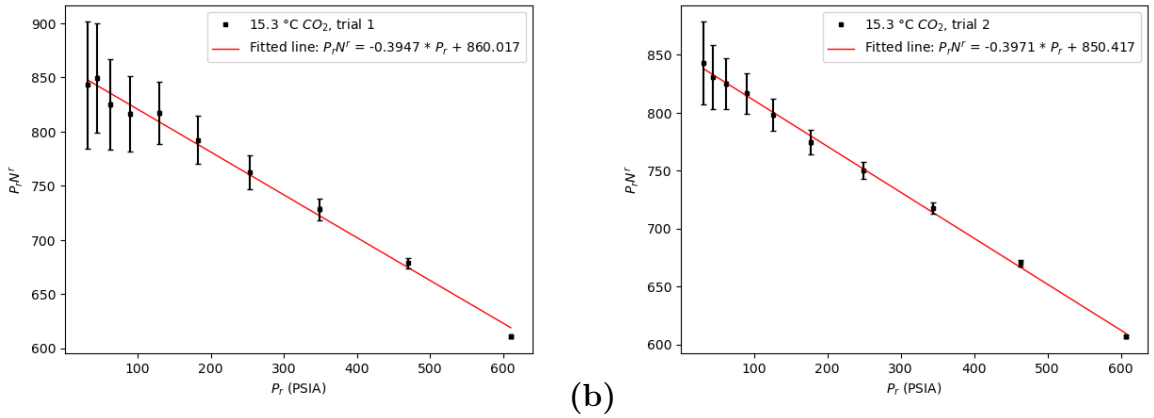

(a) (b)

Figure C4: P_rN^r as a function of pressure at 15.3°C for carbon dioxde. The linear model is fitted to the (a) first trial and (b) second trial to determine the initial compressibility factor Z_0. The vertical error bars represent the propagated error of P_rN^r and the horizontal error bar represents the measured uncertainty of the pressure.

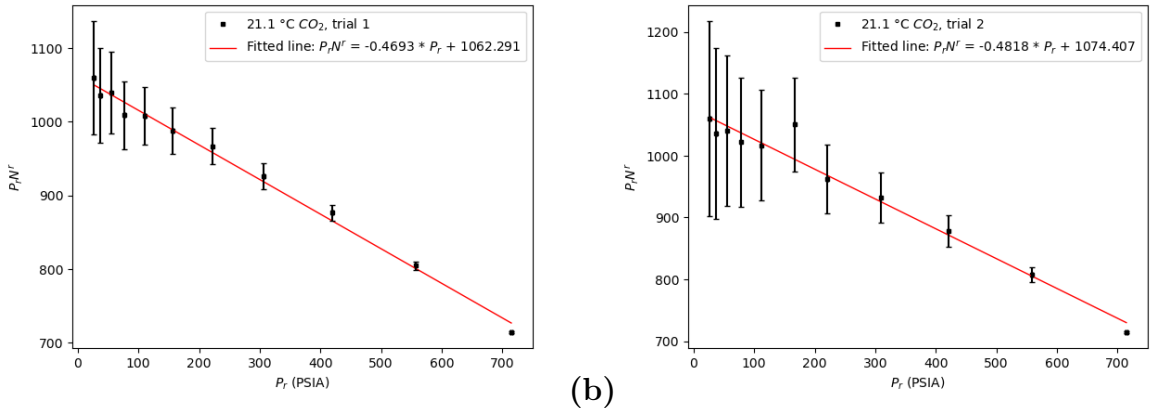

(a) (b)

Figure C5: P_rN^r as a function of pressure at 21.1°C for carbon dioxide. The linear model is fitted to the (a) first trial and (b) second trial to determine the initial compressibility factor Z_0. The vertical error bars represent the propagated error of P_rN^r and the horizontal error bar represents the measured uncertainty of the pressure.

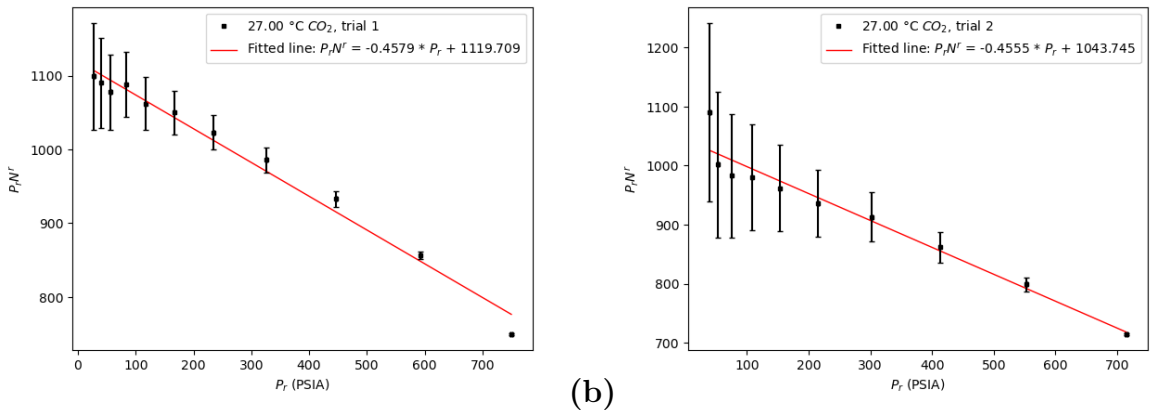

(a) (b)

Figure C6: P_rN^r as a function of pressure at $27°C$ for carbon dioxide. The linear model is fitted to the (a) first trial and (b) second trial to determine the initial compressibility factor Z_0. The vertical error bars represent the propagated error of P_rN^r and the horizontal error bar represents the measured uncertainty of the pressure.

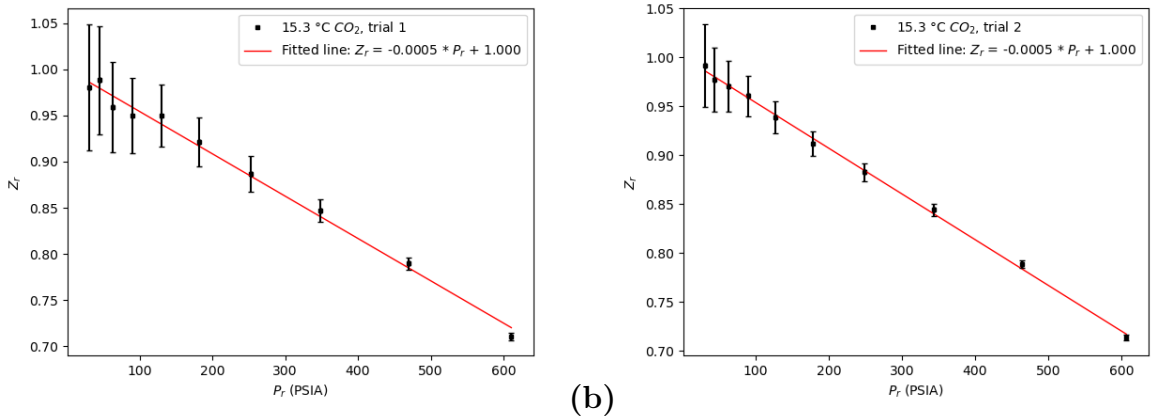

(a) (b)

Figure C7: Z_r as a function of P_r at 15.7°C for the (a) first and (b) second trial for carbon dioxde. Vertical error bars represent the propagated error in Z_r. The pressure error is 1 psi from measurement.

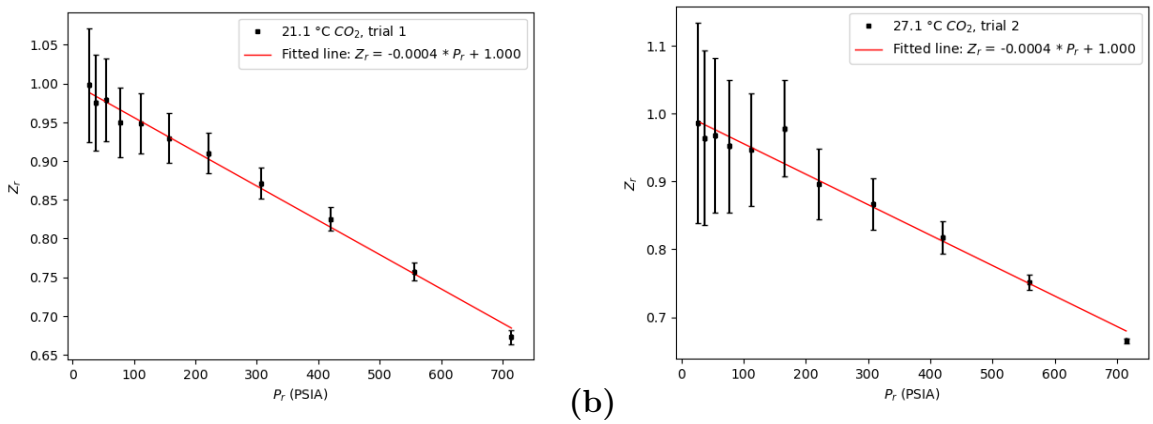

(a) (b)

Figure C8: Z_r as a function of P_r at 21.1°C for the (a) first and (b) second trial for carbon dioxde. Vertical error bars represent the propagated error in Z_r. The pressure error is 1 psi from measurement.

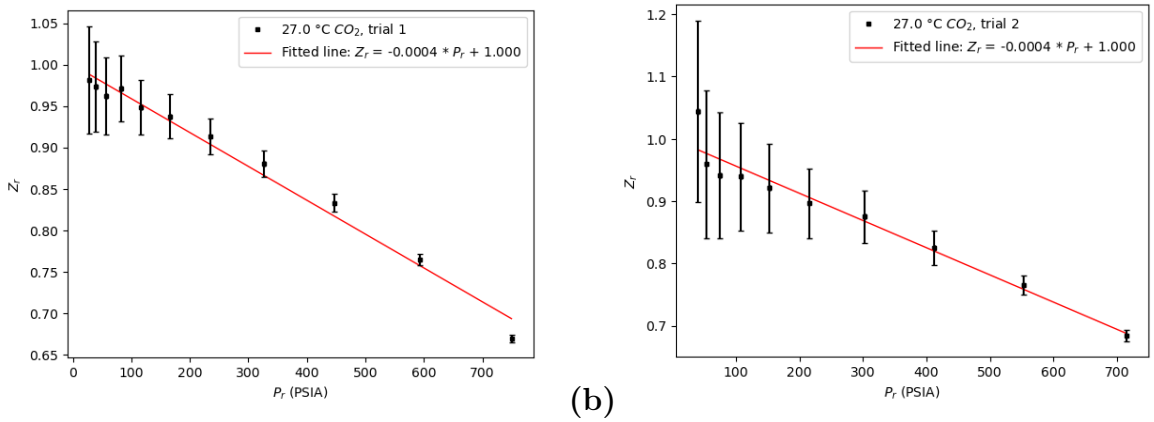

(a) (b)

Figure C9: Z_r as a function of P_r at 27.0°C for the (a) first and (b) second trial for carbon dioxde. Vertical error bars represent the propagated error in Z_r. The pressure error is 1 psi from measurement.

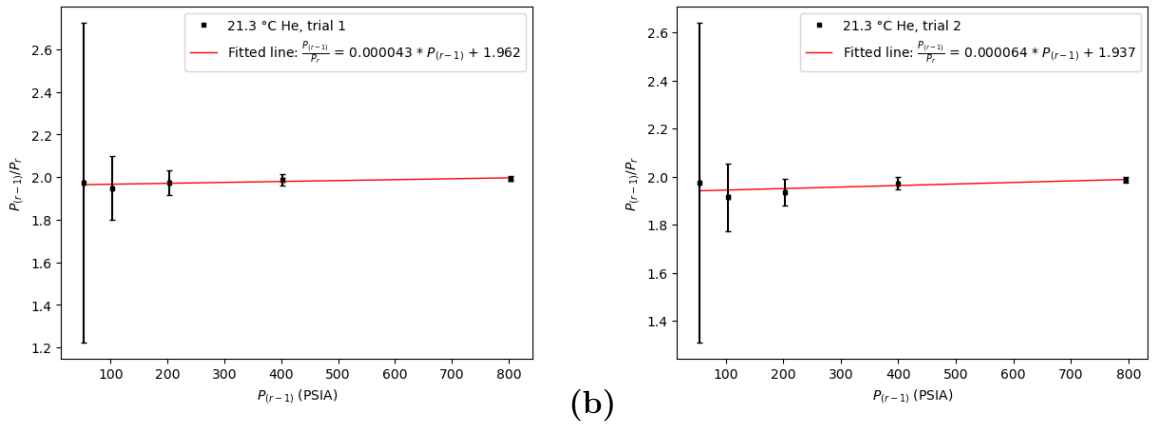

(a) (b)

Figure C10: $\frac{P_{r-1}}{P_r}$ as a function of P_{r-1} of helium at 21.3°C. The linear model is fitted to the (a) first trial (b) second trial to determine the pressure decrease as pressure approaches zero. The vertical error bars represent the propagated error of $\frac{P_{r-1}}{P_r}$ and the horizontal error bar represents the measured uncertainty of the pressure

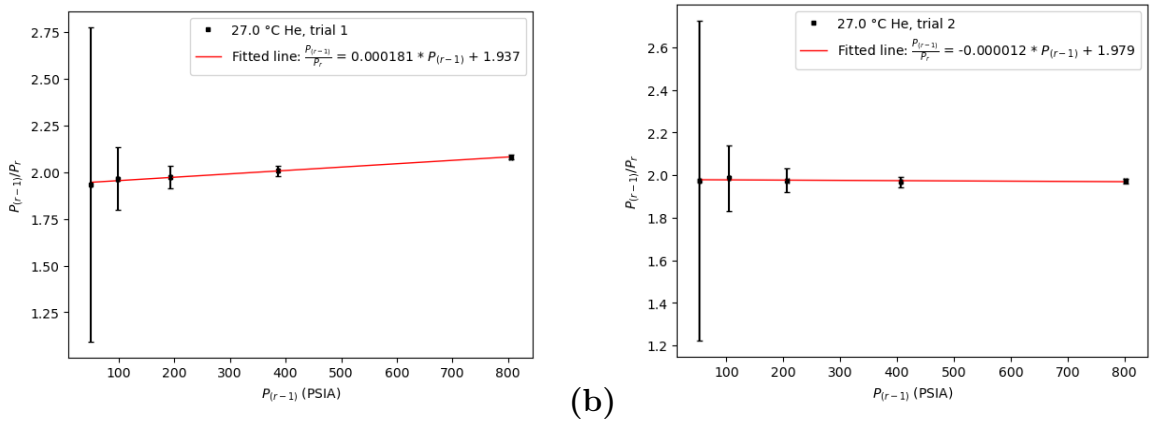

(a) (b)

Figure C11: $\frac{P_{r-1}}{P_r}$ as a function of P_{r-1} of helium at 27.0°C. The linear model is fitted to the (a) first trial (b) second trial to determine the pressure decrease as pressure approaches zero. The vertical error bars represent the propagated error of $\frac{P_{r-1}}{P_r}$ and the horizontal error bar represents the measured uncertainty of the pressure

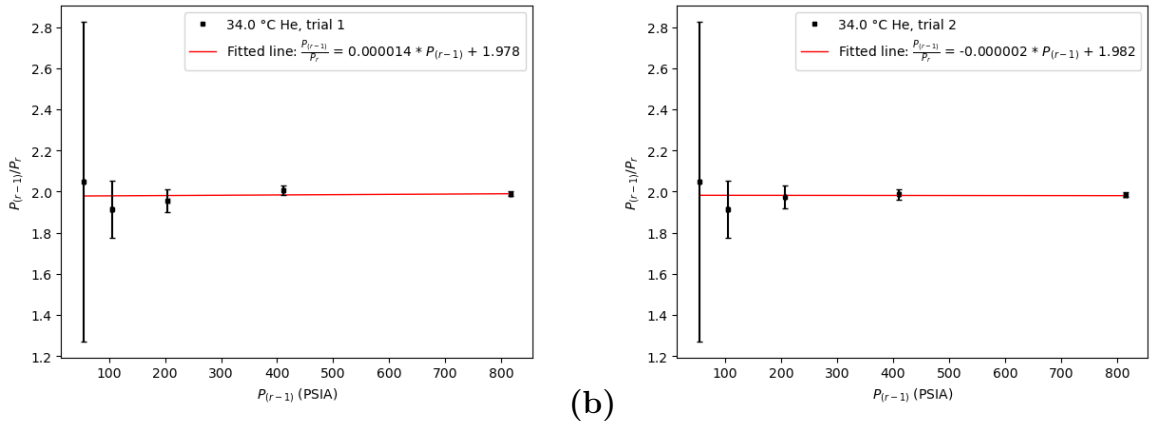

(a) **(b)**

Figure C12: $\frac{P_{r-1}}{P_r}$ as a function of P_{r-1} of helium at $34.0°C$. The linear model is fitted to the (a) first trial (b) second trial to determine the pressure decrease as pressure approaches zero. The vertical error bars represent the propagated error of $\frac{P_{r-1}}{P_r}$ and the horizontal error bar represents the measured uncertainty of the pressure

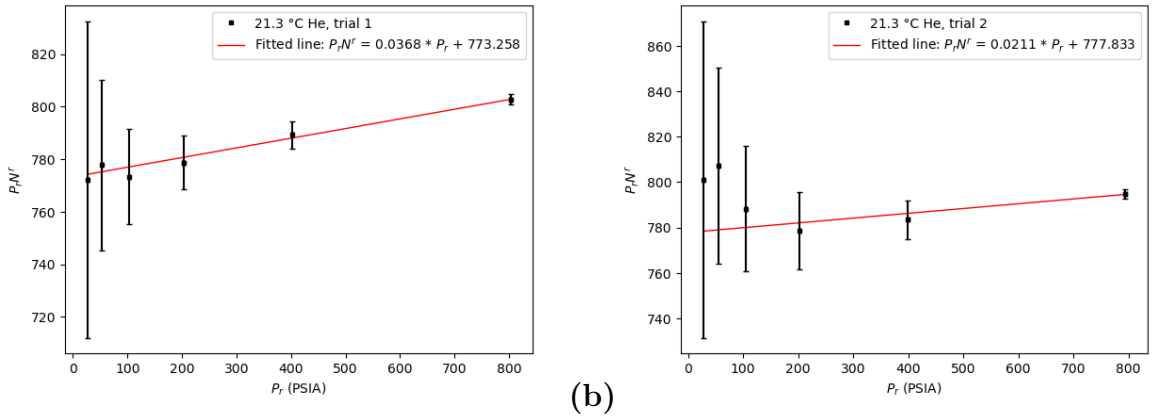

(a) **(b)**

Figure C13: P_rN^r as a function of pressure at $21,3°C$ for helium. The linear model is fitted to the (a) first trial and (b) second trial to determine the initial compressibility factor Z_0. The vertical error bars represent the propagated error of P_rN^r and the horizontal error bar represents the measured uncertainty of the pressure.

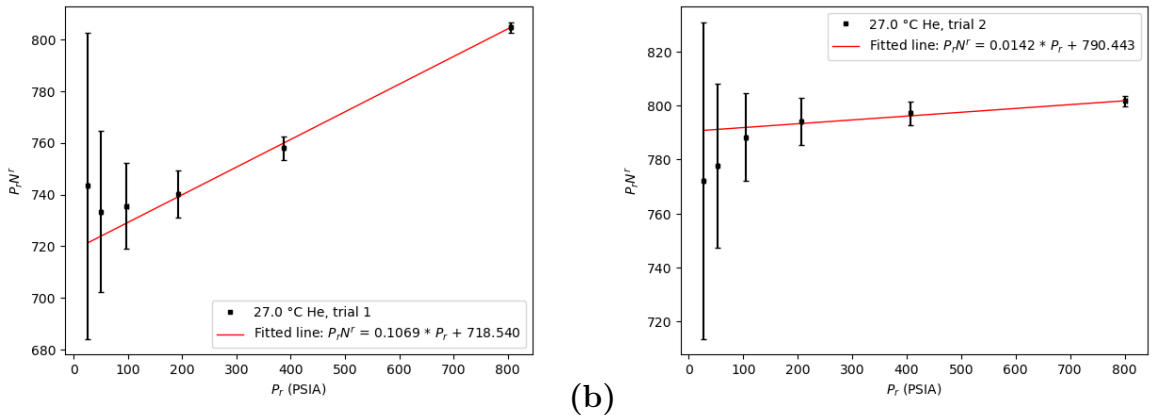

(a) **(b)**

Figure C14: P_rN^r as a function of pressure at $27.0°C$ for helium. The linear model is fitted to the (a) first trial and (b) second trial to determine the initial compressibility factor Z_0. The vertical error bars represent the propagated error of P_rN^r and the horizontal error bar represents the measured uncertainty of the pressure.

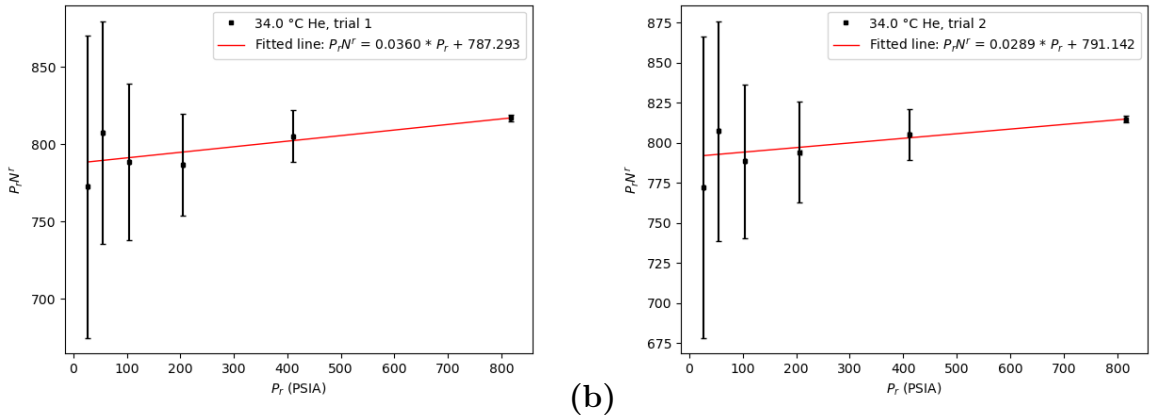

(a) (b)

Figure C15: P_rN^r as a function of pressure at 34.0°C for helium. The linear model is fitted to the (a) first trial and (b) second trial to determine the initial compressibility factor Z_0. The vertical error bars represent the propagated error of P_rN^r and the horizontal error bar represents the measured uncertainty of the pressure.

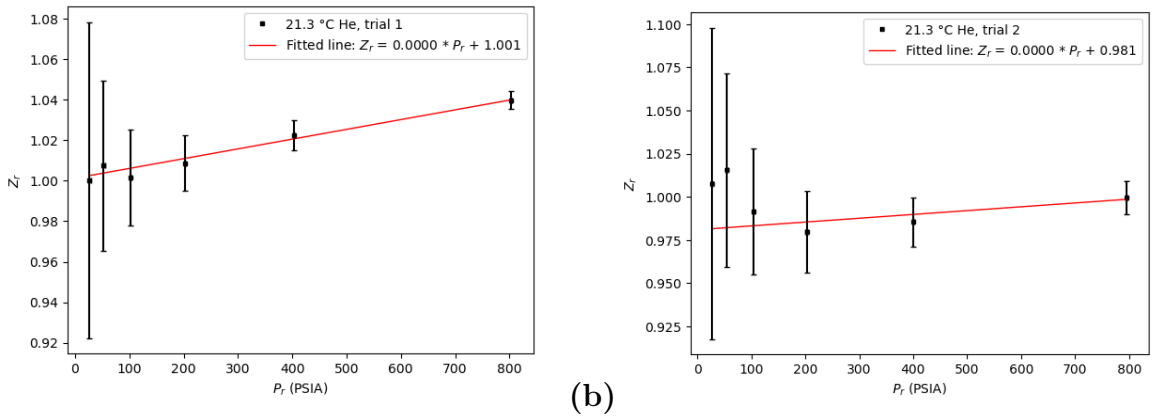

(a) (b)

Figure C16: Z_r as a function of P_r at 21.3°C for the (a) first and (b) second trial for helium. Vertical error bars represent the propagated error in Z_r. The pressure error is 2 psi from measurement.

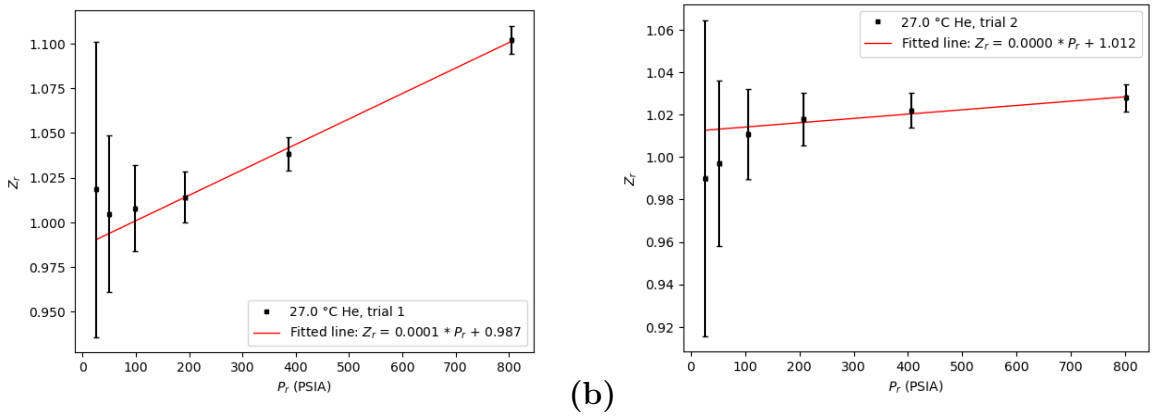

(a) (b)

Figure C17: Z_r as a function of P_r at 27.0°C for the (a) first and (b) second trial for helium. Vertical error bars represent the propagated error in Z_r. The pressure error is 2 psi from measurement.

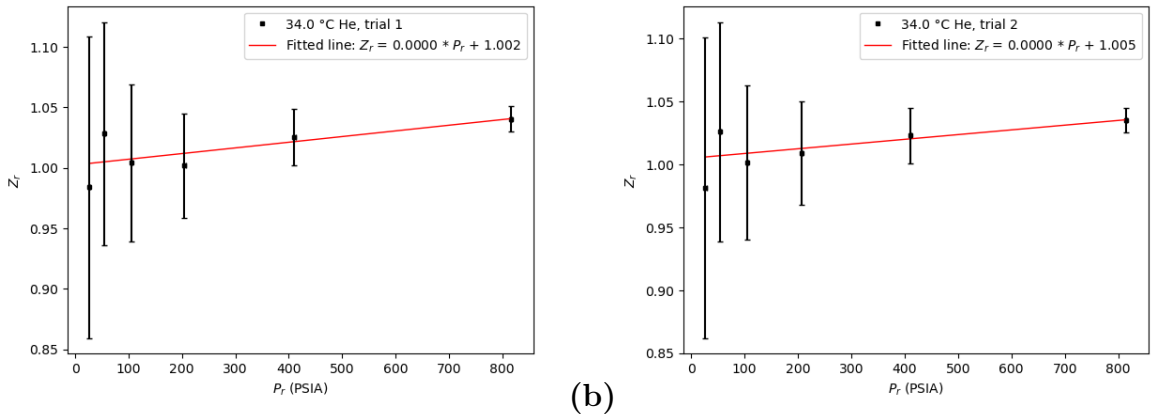

(a) **(b)**

Figure C18: Z_r as a function of P_r at 34.0°C for the (a) first and (b) second trial for helium. Vertical error bars represent the propagated error in Z_r. The pressure error is 2 psi from measurement.

Table C.1[9]: Literal second virial coefficients value of helium at different temperatures

Temperature (K)	B (cm^3/mol)
200	12.33
250	12.16
300	11.95
350	11.73

Table C.2[11]:Literal second virial coefficients value of carbon dioxide at different temperatures

Temperature(K)	B (cm^3/mol)
283	-136.7
299.5	-120.5
309.5	-111.3

D program file

```python
import pandas as pd
import numpy as np
import matplotlib.pyplot as plt
from scipy.optimize import curve_fit
from scipy.stats import chi2

# Define the linear model for curve fitting
def linear_fit(x, a, b):
    return a * x + b

# Plotting, fitting, and calculating chi-squared
def plot_and_chi_squared(pr_sets, zr_sets, zr_err_sets, temperature, marker, color):
    # Concatenate all data points and errors for current temperature
    pr_data = pd.concat(pr_sets).to_numpy().flatten()
    zr_data = pd.concat(zr_sets).to_numpy().flatten()
    zr_err = pd.concat(zr_err_sets).to_numpy().flatten()

    # Clean data to remove NaNs and Infs
    valid_indices = ~np.isnan(pr_data) & ~np.isinf(pr_data) & ~np.isnan(zr_data) & ~np.isinf(zr_data) & ~np.isnan(zr_err) & ~np.isinf(zr_err)
    pr_data = pr_data[valid_indices]
    zr_data = zr_data[valid_indices]
    zr_err = zr_err[valid_indices]

    # Perform the fit
    popt, pcov = curve_fit(linear_fit, pr_data, zr_data, sigma=zr_err, absolute_sigma=True)

    # Generate x values for the fit line
    pr_line = np.linspace(pr_data.min(), pr_data.max(), 100)
    zr_line = linear_fit(pr_line, *popt)

    # Plotting
    line_label_2 = f'{temperature}°C He'
    line_label_1 = f'{temperature}°C Fit: $Z_{{r}}$ = {popt[0]:.6f}$P_{{r}}$ + {popt[1]:.4f}'
    plt.errorbar(pr_data, zr_data, yerr=zr_err,xerr=2, fmt=marker, color=color, label=line_label_2, capsize=1.5)
    plt.plot(pr_line, zr_line, '--', color=color, label=line_label_1)

# Set up the plot
plt.figure(figsize=(10, 8))

# Call the plotting function for each temperature set with specific markers and colors
plot_and_chi_squared(pr_34_sets, zr_34_sets, [zr_34_1_err, zr_34_2_err], '34', '^', 'olive')
plot_and_chi_squared(pr_27_sets, zr_27_sets, [zr_27_1_err, zr_27_2_err], '27', 's', 'red')
plot_and_chi_squared(pr_21_sets, zr_21_sets, [zr_21_1_err, zr_21_2_err], '21', 'o', 'teal')

# Plot details
plt.xlabel('$P_{{r}}$ (PSIA)')
plt.ylabel('$Z_{{r}}$')
plt.legend()
plt.show()
```

Figure D19: sample program file for Chi-Square implementation.

```python
# Second Virial
temperatures = np.array([300.15,294.15,288.15])  # Temperatures in Kelvin
B_values = np.array([-172.6431207,-175.6183697,-168.3190103])  # B values
B_errors = np.array([7.244428396,7.100290681,6.955437816])  # Errors in B values, optional

def linear_fit(x, a, b):
    return a * x + b

# Perform curve fitting using the least squares method
popt, pcov = curve_fit(linear_fit, temperatures, B_values, sigma=B_errors)

# Generate points for the regression line
temp_fit = np.linspace(min(temperatures), max(temperatures), 100)
B_fit = linear_fit(temp_fit, *popt)

# Create the plot
plt.figure(figsize=(8, 6))
plt.errorbar(temperatures, B_values, yerr=B_errors,xerr=0.5, fmt='o', capsize=5, label='Second Virial Coefficient, B')
plt.plot(temp_fit, B_fit, 'r-', label='Fit: {:.2f} * T + {:.2f}'.format(*popt))
# Customizing the plot
plt.xlabel('Temperature (K)')
plt.ylabel('Second Virial Coefficient, B')
plt.legend()
# Show the plot
plt.ylim(-200,-150)
plt.show()

import numpy as np
import scipy.stats as stats

# Values from the provided image
image_temperatures = np.array([200, 250, 300, 350])
image_B_values = np.array([12.33, 12.16, 11.95, 11.73])

temperatures = np.array([300.15, 294.15, 288.15])  # Your experiment temperatures
B_values = np.array([-172.6431207, -175.6183697, -168.3190103])  # Your experiment B values

# Interpolating your data to find B values at temperatures 300 K
from scipy.interpolate import interp1d

interp = interp1d(temperatures, B_values, kind='linear', fill_value="extrapolate")
experiment_B_at_image_temps = interp(image_temperatures)

# T-test
t_stat, p_value = stats.ttest_ind(experiment_B_at_image_temps, image_B_values, equal_var=False)

print("T-statistic:", t_stat)
print("P-value:", p_value)
```

Figure D20: sample program file for t-test conducted of second virial coefficients for helium with literal values.